Iran University of Science and Technology

International Journal of

Railway Research

Using low-cycle fatigue method to predict fatigue life of rail crack initiation location by means of 3D-finite element simulation on sharped curved track

Amin Nazari[1*], Dr. Parisa Hosseini Tehrani[2]

[1]School of Railway Engineering, Iran University of Science and Technology, Tehran 16846-13114, Iran, nazari_amin@rail.iust.ac.ir

[2]Associate Professor, School of Railway Engineering, Iran University of Science and Technology, Tehran 16846-13114, Iran, Hosseini_tiust@iust.ac.ir

ARTICLE INFO

Article history:
Received: 06.18.2023
Accepted: 07.15.2023
Published: 07.23.2023

Keywords:
Dynamic modelling
wheel-rail interaction
sharped curved track
critical plane method
low cyclic fatigue

A B S T R A C T

Analysis of wheel-rail interaction is considerable in dynamic issues specially on sharped curved track of railway systems. Both location and magnitude of wheel-rail stress must be appraised in a well-way and correctly via computational aid. In curved- tracks, evaluation of the force applied on the wheel is complex is multiaxial rather than uniaxial; thus, a more complete analysis is required. In current paper, a reliable numerical approach is made to investigate fatigue crack initiation life on sharp curved tracks by combining Universal Mechanism software to state the distribution of axial wheel force and a comprehensive three-dimensional finite element simulation to get the resulting stress at the wheel-rail interaction area. low cyclic fatigue situation method based on and multiaxial loading is used for determining the fatigue life cycle. The effect of radius and on sharped curved track under three contact situation high adhesion, low adhesion was studied. The present analysis predicts rational wheel-rail dynamic response to cyclic loading effectively.

1. Introduction

though static condition in railways problems assign some understanding into the issue [1], dynamic contact problems are more high-priority.

Thus, RCF in railway transportation plays a key role on the operation cost and safety passenger. In curved railways, adhesion and the radius of curvature, length of the radius curved section effect on the dynamic load, cause the problem even more elaborated.

Hybrid exhibited, physics-informed statistical model introduced by Gao et al, crack formation and wear occur more on curvature with less radius [2].

Multibody dynamic modeling of the wheel-rail system requires reliable calculation of the contact area features. The constraint approach and elastic formulation are the two main methods of contact point detection, considering 5 and 6 degrees of freedom (DOFs) for each body [3].

Matsumoto et.al by means of experimental method measure the contact forces. the lateral

*Corresponding author
Email address: nazari_amin@rail.iust.ac.ir

[DOI: 10.22068/ijrare.314]

fluctuation of wheel measured with non-contact gap sensors.[4]. Numerical studies on this subject have been performed extensively[5].

In realistic conditions, a spectrum of load is applied to the system with variable amplitude and frequency. Multi-dynamic simulation (MDS) software such as Universal Mechanism (UM) has been used for this matter [2].

Furthermore, numerical methods as like finite element method are appropriate method to study wheel and rail interaction to determine phenomenon exactly also is suitable for predicting fatigue life crack initiation.[6], this research focus is on developing fatigue damage models for wheel-rail interaction.

In order to study change of stress and strain of the railhead made happen by global bending and local contact forces, a tool was developed by Ringsberg et al comprised of track and rail FE models [7]. A realistic load of a commuter train traffic was applied to the model and two fatigue crack initiation criteria were compared. Low-cycle fatigue criterion predicted the minimum number of cycles at which crack initiation occurred, while ratchetting criterion was employed at high cycles since ratchetting material response was distinguished after 16-wheel passages. Their simulation results for the orientation of crack initiation were consistent with the data measured in Sweden.

In[8]Jiang et al. integrated strain-rate effect, statistics, and probabilistic method in a two-dimensional FE model to study the wheel-rail RCF. They found that rail crack propagation in low-speed trains began in an opening mode and developed in a sliding one. While in high-speed trains, the crack always propagated in the opening mode.

It is well-accepted by Chaboche & Lemaitre simulation that in the critical plane the potential of fatigue crack initiation is severe [9]. Using Finite Element method beside the critical plane results in precise prediction of fatigue crack situation [10]. Their model predicts an S-shaped probability curve for fatigue crack initiation life versus traffic volume. The valuable outcome in this curve was as follows. The rail fatigue cracks would not occur when fatigue properties reached a certain level. combining finite element with other theory as like SWT, critical plane is common to evaluate the exact fatigue life and crack orientation [11]. [12] also In other work, El-Sayed et al combine finite element method with critical plane method to determine exact crack situation on railway[13]. In claimed that considering an explicit solution instead of an implicit one, presuming elastic-plastic material properties instead of elastic ones, and including the global bending effect on local material response led to realistic results. Their numerical procedure was validated with field observations and estimated 70 days as crack initiation life [13].

The foresaid above numerical studies chiefly perform on straight tracks. However, the complicated conditions of the curved also model with the FE method for three cases of new wheel/new rail, new wheel/worn rail, and worn wheel/worn rail by Vo et al [14].

Despite all the mentioned research, the stress analysis on low rails of the curved tracks under fatigue condition has not yet been accurately investigated. In this work, a comprehensive 3D elastic-plastic FE model and MDS method included the first wheel on the curved low track is simulated. Fatigue is simulated by 12 cycles of the wheel passage. For each wheel passage, the time-dependent multiaxial load on the wheel is obtained from UM software. Contact pressure and stress distribution within the wheel-rail contact patch are then measured by Abaqus software and life fatigue crack initiation plane is identified using SWT parameter. The effect of important Parameter is also studied on curved track, rail radius and the amount of adhesion under three contact situation high adhesion, low adhesion. It should be noted that the rail cant and angle of attack (AOA) is included in our model.

2. Approach

2.1. Establishment of dynamic and finite element model and its verification

To achieve an accurate insight into the wheel-rail contact zone, the load applied to the center of the wheel is acquired with MDS method, specifically with UM software. In UM software, the multi-body dynamic model of the vehicle is developed, including the car body, 2 bogies, and 6 wheelsets. All of the aforementioned components are considered to be rigid with 5 DOFs. Primary and secondary suspension

[DOI: 10.22068/ijrare.314]

systems are applied to the model as well. Spring-damper elements assume to simulate the primary suspension system between the two bogies and six wheelsets and the secondary suspension system between the car body and two bogies. Selecting the characteristics of the wheel and rail are based on the Iranian railway network, so S1002 and UIC60 profiles are used, respectively. It should note our study scope for evaluating life fatigue crack initiation is 60cm of the length curved low track and specially the results got of UM because of the damage show more at the entrance railway due to force fluctuation in three dimension. The load (longitudinal, lateral, and vertical forces obtain from the UM simulation) and the gravitational force apply on the geometric center of the wheel as reference node which couple with inside surface of the wheel

The wheel velocity is assumed to be 80 km/h. considering a cant of 2.86˚ and angle of attack 1/3° and three different radii of 200,300, 500, and tangent rail under low adhesion μ=0.2 and high adhesion μ=0.45, The mechanical specification of the wheel and rail addressed in Table 1.The procedure of MDS followed in this study was verified with the information available in UM help [15, 16].

The wheel and rail geometry profiles play a critical role in defining the contacting surface constraints, which directly influence changes of stress distribution and contact pressure at the contact zone. Thus, geometric characteristics should be precisely specified. Moreover, the boundary conditions at the contact region must carefully define. Selecting the optimum simulation procedure and studying the effect of different factors on the contacting wheel and rail is essential in finding accurate results. In this work, because of get more exact result we simulate 3D FEM in Abaqus software. the length of curved track is 60cm (Fig.1). every analysis includes of 12 pass and load versus of time apply to the model considered. employing UM software to calculate the dynamic force utilize on the wheel during the simulated length of the rail (60 cm). Various curvatures, slip rations are employed to the model to examine their effect on SWT parameter. It is well-known that the effect of curvature alters the loads exerted on the wheel. Besides, the contact position and stress distribution will change due to cant effects.

For modeling the fastening system (the rail pad, sleeper, and ballast.) In this simulation at the beginning and end of the rail Two groups of spring-damper elements are considered. The friction coefficient between the wheel and rail is $\mu = 0.2$ and $\mu = 0.45$.

2.2. Mesh convergence evaluation

In this study, several stresses and strains needed to seizure the contact area. So, in this simulation used different meshing size to optimize solution time and access logical result total length of simulated rail is 60cm and in middle of rail meshed finer and other segment of sample a coarse mesh assigned (Fig. 1C). By considering the fully integrated eight-node linear brick (C3D8) elements, the mesh convergence is achieved with a combination of coarse and fine elements. for comparing result and access the best size for meshing to saving run time a mesh sensitivity was done refines to get to an optimized mesh. It should note that the mesh size at the lower segment of the wheel is changed since it affected the stresses and strains of the railhead. Computational time and maximum contact pressure are determined for five different element sizes, as shown in Table 3. As the mesh becomes finer, the maximum contact pressure increases. The highest maximum contact pressure is 1031 MPa for 1.6×1.6 mm mesh. However, this value altered by less than 1% for 2×2 mm mesh (1025 MPa). so, the optimum meshing size obtains 2×2 mm and the run time decrease about 1/9 while the difference contact pressure less than 1%. Hence, to achieve both acceptable accuracy and appropriate time consumption, 2×2 mm mesh is chosen for further investigation. In this model, the total number of elements and nodes were 8666747 and 8984867, respectively.

To verify the precision of output of simulation including contact area, von Mises stress, and contact pressure compared in table 2 the results are compared in A-axis is direction of movement and B-axis is lateral direction, the difference between the two study are 4% and 4.2%. The maximum contrast of von Mises stress and contact pressure between our simulation and the reference were 9% and 5.4%, respectively.

[DOI: 10.22068/ijrare.314]

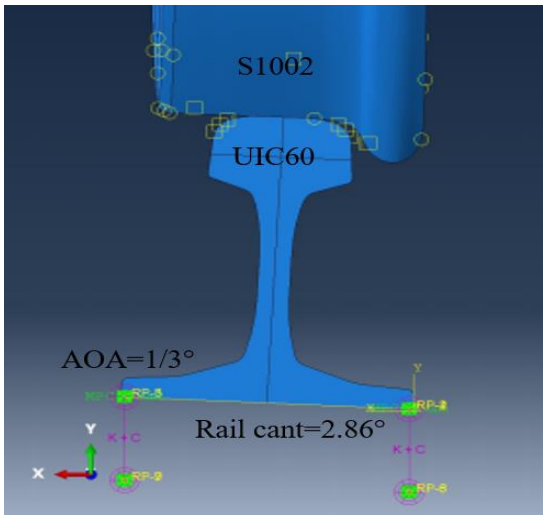

(A)

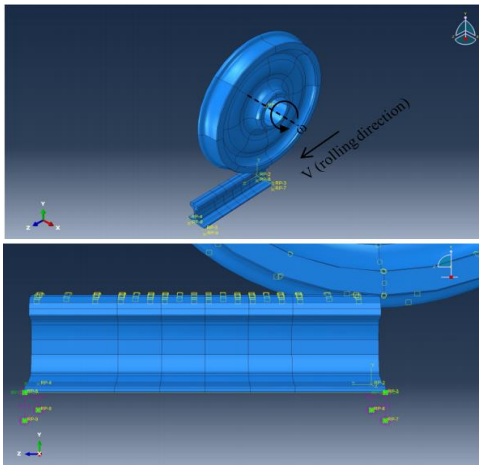

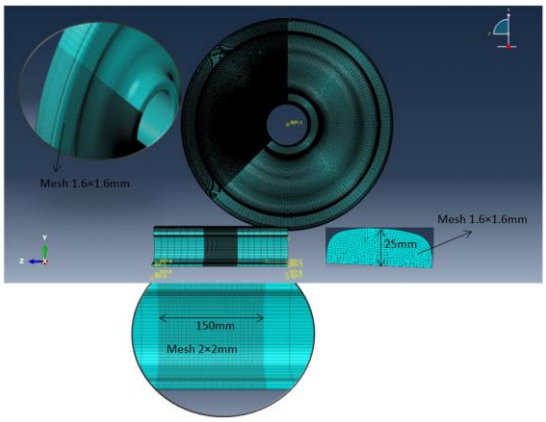

(B) (C)

Figure 1. **(**A) 3D FE model of wheel-rail interaction produced by Abaqus software. the position of the left wheel-rail simulation wheel-rail in X-Y (B) and Y-Z planes are provided as well (C) Overall dimension meshing for simulation of the simulation.

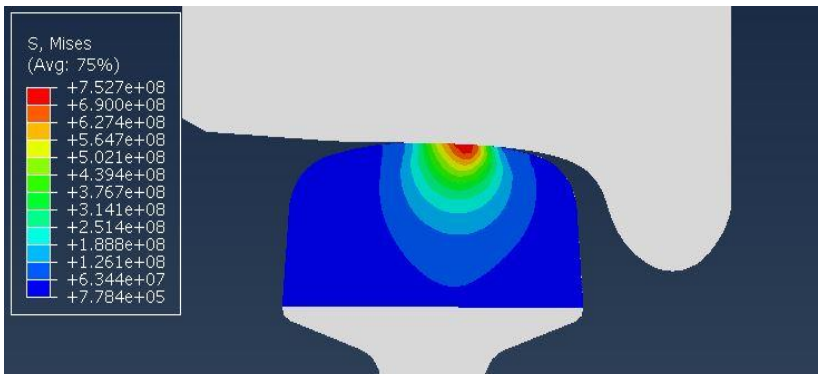

Figure 2. The von Mises stress distribution achieved according to the input data provided in [14, 17]

[DOI: 10.22068/ijrare.314]

Table1. Required data for modeling of the interaction of wheel and curved track contact and fatigue parameter[18]

Parameter		**value**
Loading parameter		
Overall mass and velocity (the Iranian railway)	M	149.6 ton
	V	80 km/h
Suspension system	K_1	1.15 MN/m
	C_1	2500 kNs/m
Rail and wheel characteristics	*Rail*	UIC60 (900A)
	Wheel	S1002
Track parameters		
Fastening system	K_2	1300 MN/m
	C_2	45 kNs/m
Rail pad	E	800 Gpa
	ϑ	0.46
	ρ	950 kg/m^3
Sleeper	E	20.3 Gpa
	ϑ	0.21
	ρ	115.7 kg/m^3
Ballast	K_3	45 MN/m
	C_3	23 kNs/m

The Constant for Determining Crack Initiation Life

Parameter	$\gamma_1, \gamma_2, \gamma_3$	C_1, C_2, C_3	R	Q_∞	σ_f'	ε_f'	τ_f'	γ_f'	J	b
Value	55, 600, 2000	24750, 60000, 200000	500	$-189\ Mpa$	$936\ Mpa$	10.6%	$468\ Mpa$	15.45%	0.2	-0.089

Table 2. Convergence study of the mesh. Different mesh sizes ranging from 1.6 mm to 5 mm were applied to the .model and the resulting maximum contact pressure was chosen as the determining parameter

	Number of elements	**Number of nodes**	**Element types**	**Run time(hr)**	**Contact pressure(mpa)**	**difference**
Mesh 1.6mm	8666747	8984867	C3D8R DASHPOTA MASS RNODE3D SPRINGA	138	1025	<1%
Mesh 2mm	5602356	5865067	C3D8R DASHPOTA MASS RNODE3D SPRINGA	113	1015	2%
Mesh3mm	2547851	2784158	C3D8R DASHPOTA MASS RNODE3D SPRINGA	92	960	6%
Mesh 5mm	620540	692946	C3D8R DASHPOTA MASS RNODE3D SPRINGA	72	920	10%

Table 3. errors between the values calculated by the current simulation and the work of [9] for major and minor axis of the elliptic contact area, maximum contact pressure, and maximum von Mises stress. Error is less than 10% for all the parameters, showing good agreement between the models.

Approach		Presented Dynamic FE model	Ref [9]	Diff. between [9] and dynamic FE model (%)
Contact patch	length of e longitudinal direction A(mm)	19.96	20.8	**4**
	length of latera direction B (mm)	13.6	14.2	**4.2**
Maximum contact pressure B (MPa)		984	1091	**9**
maximum von-Mises stress (MPa)		752	795	**5.4**

[DOI: 10.22068/ijrare.314]

3. Methods

As said earlier, our simulation considers dynamic load by taking into account 12 pass on a curved track. so, the combination of the multiaxial low cycling fatigue (LCF) mode [9, 12, 13]l and the Strain-life fatigue properties, which are also often referred to as "low-cycle fatigue is used to examine the life of fatigue crack initiation, The model presented by Smith, Watson, and Topper (often called the "SWT parameter"), based on strain-life test data obtained with various mean stresses) is adopted in this study as follows:

$$\sigma_{max}\varepsilon_a E = \left(\sigma_f{}'\right)^2\left(2N_f\right)^{2b} + \sigma_f{}'\varepsilon_f{}'E\left(2N_f\right)^{b+c} \quad (1)$$

With as the $\sigma_{max} = \sigma_m + \sigma_a$ and ε_a is alternating strain. With σ'_f, ε'_f,, b, and c as material constant in Table 4.

4. Results

4.1 Contact pressure and stress distributions within the contact zone

Due to considering the effects of residual stress, the results are considered for twelve-wheel passes. zone obtains with the aid of the FE simulation, the contact pressures and the von Mises stresses evaluate within the contact zone. It should emphasize there is only one point between the wheel and the rail .The hunting motion on curved track is responsible for altering the multiaxial forces applied to the contact zone. The Mises stress changes is shown in the Fig. 3A, with the upmost value of 791 MPa for R=200 m and slip ratio=٥٪, The stress tensor is non-proportional at the contact zone. The effect of pass radius and adhesion on the maximum von Mises stress and contact pressure is similar. distribution the contact pressure. change of contact pressure along the rolling direction versus the curvature radius and slip ratio are evaluated, and the results are showed in Fig. 3B, C. According to this figure, As the radius of the track decreases and the amount of surface adhesion increases, the amount of contact pressure and the numerical value of maximum von Mises stress increase.

4.2. Fatigue life parameter calculation

The last step was evaluating fatigue life of fatigue crack initiation based on the obtained stress and specifying the maximum von-misses stress, and. Tables 4 demonstrate the magnitudes of N_f and the points at which $\sigma_{mises-max}$occurred In different radii and different adhesion coefficients, the amount of the effective parameter in the life of crack initiation was checked, and therefore, with the decrease of the path radius and the increase of the amount of slip, the amount of crack initiation life increases. and the possibility of cracking increases.

Table 4. Change of N_f curvature radius and adhesion

		Straight Radius	*Radius (m)*		
			500	*300*	*200*
High adhesion μ=0.45	**N_f (10^6)**	0.25	0.22	0.17	0.11
	S-Mises (MPa)	654	690	721	791
High adhesion μ=0.2	**N_f (10^6)**	0.68	0.45	0.41	0.31
	S-Mises (MPa)	489	520	590	615

5. Discussion

In this research, wheel-rail interaction numerically explorers to NFL Check the fatigue crack initiation life. The numerical procedure included estimating time-dependent multiaxial load acting on the wheel using UM software, obtaining contact pressure and von Mises stress distributions at the wheel-rail contact patch using FE simulation, and evaluating fatigue life crack initiation parameters. In the used FE method, an explicit elastic-plastic algorithm is considered. Furthermore, parametric studies

[DOI: 10.22068/ijrare.314]

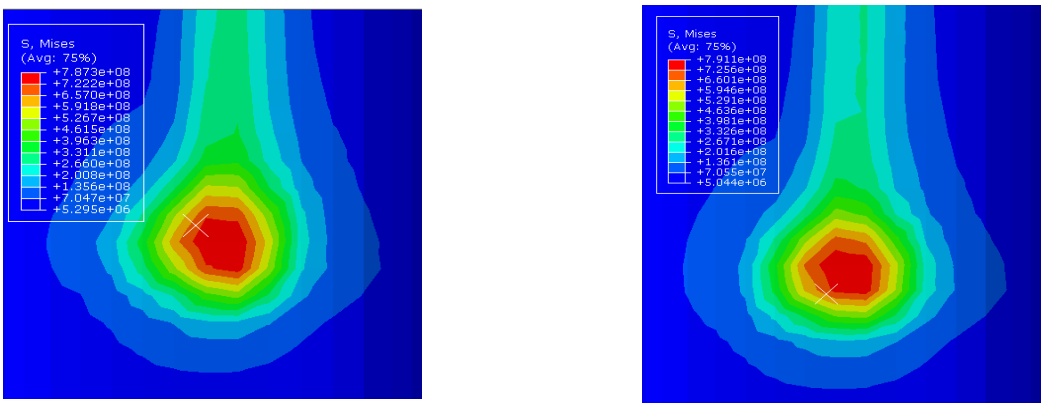

(A)

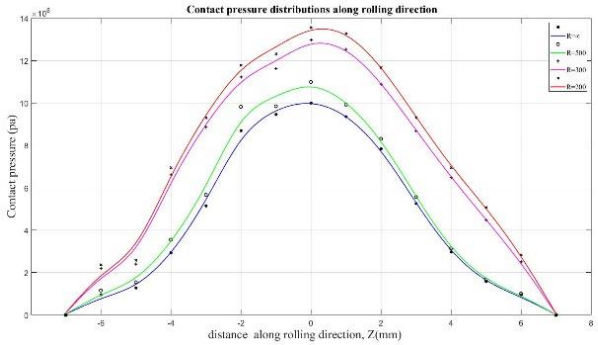

(B)

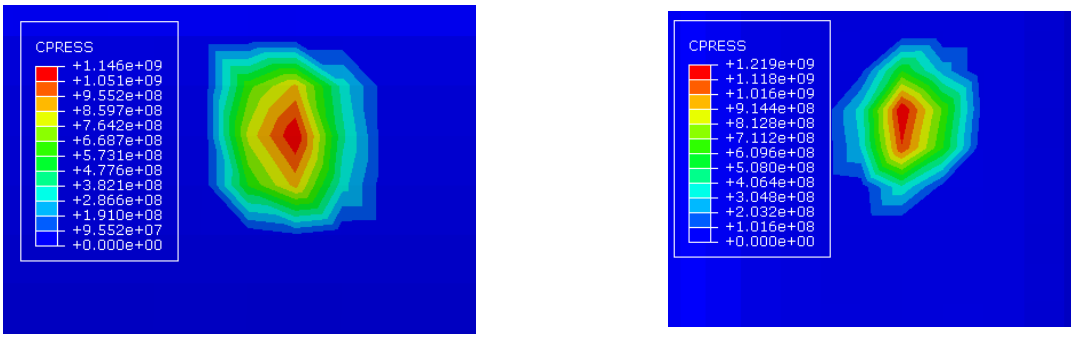

(C)

Figures 3. (A) the Variations of von Mises stress and shape of the contact area in the radius 300m of the low rail, (B) The effect of the radius of curvature of the track on the contact pressure in the direction of movement and (C). Contact pressure changes on the low rail within the contact area. Elliptical contact zone for R=300 m and slip ratio=5%

are performed on the effect of the curvature radius of the rail, slip ratio The results are defined as follows

1. By reducing the radius of curvature of the track and increasing the surface adhesion, the shape of the contact area does not become fully oval.
2. The radius of curvature of the path is an effective parameter for changes in crack initiation life (N_f). According to the investigations carried out in this research,

[DOI: 10.22068/ijrare.314]

the amount of difference in Mises stress and crack initiation life compared to the curved path is 20% and 50%

In conclusion, taking into A detailed examination of the contact between the wheel and the rail is very important to check the amount of contact stress, and it is one of the effective factors to prevent damage, especially at the entrance of curved rail tracks, as well as the effects of surface adhesion and the radius of curvature of curved tracks in changes in contact stress and life. Crack initiation is very effective.

References

1. Jagadeep, B., P.K. Kumar, and K.V. Subbaiah, Stress analysis on rail wheel contact. International Journal of Research in Engineering, Science and Management, 2018. 1(5): p. 47-52.
2. Gao, T., et al., Estimation of rail renewal period in small radius Curves: A data and mechanics integrated approach. Measurement, 2021. 185: p. 110038.
3. Marques, F., et al., A three-dimensional approach for contact detection between realistic wheel and rail surfaces for improved railway dynamic analysis. Mechanism and Machine Theory, 2020. 149: p. 103825.
4. Matsumoto, A., et al., A new measuring method of wheel–rail contact forces and related considerations. Wear, 2008. 265(9-10): p. 1518-1525.
5. Powell, A. and P. Gräbe, Exploring the relationship between vertical and lateral forces, speed and superelevation in railway curves. Journal of the South African Institution of Civil Engineering, 2017. 59(3): p. 25-35.
6. Liu, Y., B. Stratman, and S. Mahadevan, Fatigue crack initiation life prediction of railroad wheels. International journal of fatigue, 2006. 28(7): p. 747-756.
7. Ringsberg, J., et al., Rolling contact fatigue of rails—finite element modelling of residual stresses, strains and crack initiation. Proceedings of the Institution of Mechanical Engineers, Part F: Journal of Rail and Rapid Transit, 2000. 214(1): p. 7-19.
8. Jiang, X., et al., Rail fatigue crack propagation in high-speed wheel/rail rolling contact. Journal of modern transportation, 2017. 25(3): p. 178-184.
9. Ghazanfari, M. and P.H. Tehrani, Increasing fatigue crack initiation life in butt-welded UIC60 rail by optimization of welding process parameters. International Journal of Fatigue, 2021. 151: p. 106367.
10. Ringsberg, J.W., Life prediction of rolling contact fatigue crack initiation. International Journal of fatigue, 2001. 23(7): p. 575-586.
11. Jianxi, W., et al., Probabilistic prediction model for initiation of RCF cracks in heavy-haul railway. International Journal of Fatigue, 2011. 33(2): p. 212-216.
12. Xin, L., V. Markine, and I. Shevtsov, Numerical procedure for fatigue life prediction for railway turnout crossings using explicit finite element approach. Wear, 2016. 366: p. 167-179.
13. El-sayed, H., et al., Prediction of fatigue crack initiation life in railheads using finite element analysis. Ain Shams Engineering Journal, 2018. 9(4): p. 2329-2342.
14. Vo, K., et al., FE method to predict damage formation on curved track for various worn status of wheel/rail profiles. Wear, 2015. 322: p. 61-75.
15. Demmel, J.W., Applied numerical linear algebra. 1997: SIAM.
16. Torre, C.G., 04 Linear Chain of Coupled Oscillators. 2014.
17. Vo, K.D., Damage analysis of wheel/rail contact associated to high adhesion condition. 2015.
18. Ghazanfari, M. and P.H. Tehrani, Experimental and numerical investigation of the characteristics of flash-butt joints used in continuously welded rails. Proceedings of the Institution of Mechanical Engineers, Part F: Journal of Rail and Rapid Transit, 2020. 234(1): p. 65-79.

[DOI: 10.22068/ijrare.314]